JOURNAL OF GEOPHYSICAL RESEARCH, VOL. 89, NO. B12, PAGES 10,115-10,124, NOVEMBER 10, 1984

MEASUREMENT REQUIREMENTS FOR GLACIAL UPLIFT DETECTION OF NONADIABATIC DENSITY GRADIENTS IN THE MANTLE

W. Fjeldskaar

SYGNA, Balestrand, Norway

L. M. Cathles

Chevron Oil Field Research Company, La Habra, California

Abstract. Recent isotope studies have rekindled interest in the possibility that the mantle may be chemically stratified and therefore nonadiabatic. Previous calculations of the last ice age are compatible only with a $\sim 10^{22}$P mantle. Calculations of the isostatic response of an adiabatic, partially nonadiabatic, and fully nonadiabatic 10^{22}P mantle to the load cycle of the last ice age show that the uplift responses of an adiabatic and even partially nonadiabatic mantle are very different. However, geoid perturbations mask these differences, and the emergence curves of the two mantle types are nearly identical except in the regions near and under the ice loads at the early stages of isostatic readjustment. The calculations suggest that we must seek shoreline emergence data around glaciated areas more than 6000 years before present if nonadiabatic density gradients in the mantle are to be detected from emergence data.

Introduction

Isostatic adjustment following the melting of the Pleistocene glaciers provides the best information we have about the fluid properties of the earth's mantle. Two recent analyses of the available postglacial uplift data have come to similar conclusions regarding the gross fluid properties of the mantle by comparing uplift pattern to theoretical models of the earth's response to deglaciation. Cathles [1975, 1980] concluded that the isostatic adjustment data are best explained by a uniform 10^{22}P Newtonian mantle capped by a lower-viscosity asthenosphere. Peltier and co-workers have also concluded that the mantle viscosity is close to 10^{22}P, although they do not require an asthenosphere (which they replace with a 120-km-thick lithosphere) and their constraints on mantle viscosity are not as tight [Peltier and Andrews, 1976; Peltier, 1982]. The conclusions of the two analyses are similar, but there are important differences in the theoretical models used in the two analyses that affect a more refined interpretation of the uplift data.

In particular, Cathles [1975], although calculating some cases with nonadiabatic density gradients (i.e., density gradients that can affect fluid flow) in the region of mantle phase changes between 335 and 635 km below the Moho, has generally assumed that the mantle is adiabatic and has argued that isostatic adjustment data are better matched by such a model [Cathles, 1980]. Peltier [1976, 1982] (see also Peltier and Wu [1982]) has assumed the mantle to be fully nonadiabatic in all his calculations.

This can lead to significant differences in calculations where both the load cycle (glaciation followed by deglaciation) and the effects of a perturbed geoid on sea level are not taken into account and to differences that will affect more refined interpretations of mantle adiabaticity even when the load cycle and geoid perturbation are taken into account. Interest in whether the mantle is adiabatic or partially nonadiabatic has been increased by isotope studies that suggest that the upper and lower mantle may be separate chemical reservoirs that are convecting separately [cf. Allégre, 1982; Jacobsen and Wasserburg, 1979]. These conclusions have been challenged by new isotope data, however [Zindler et al., 1982]. The purpose of this paper is to lay part of the theoretical foundations for a glacial uplift test of mantle adiabaticity by pointing out where emergence data contain information regarding mantle adiabaticity.

The reason for the different assumptions that have been made in theoretical models regarding mantle adiabaticity probably resides in the methods of the model computation. Love [1911] pointed out that the equations of motion are different for elastic and viscous deformation in a gravity field. In elastic deformation, material elements carry their zero-order pressure field with them; under viscous deformation, material elements move through the zero- order pressure field. As a result, buoyant forces arise from fluid motion if there are nonadiabatic density gradients, the boundary conditions for elastic and viscous deformation differ; and two density gradients must be defined in cases where gravity perturbations affect the deformation, one for the elastic deformation which is just the actual increase in density with depth and one for the fluid deformation which is the nonadiabatic variation of density with depth. (See Cathles [1975] especially pp. 11-15 for discussion of the elastic and viscous equations of motion, pp. 16-20 for the boundary condition implications, and pp. 60-71 for discussion of nonadiabatic density gradients and their effect on isostatic adjustment.)

The different elastic and viscous equations of motion pose difficulties for the straightforward application of the correspodence principle in calculating the viscoelastic response of a self-gravitating body such as the earth. It is not clear how the correspondence principle

Paper number 4B0955.
0148-0227/84/004B-0955$05.00

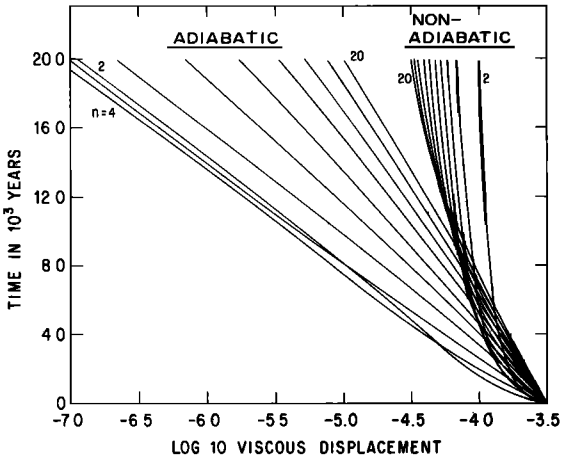

Fig. 1. Viscous decay spectrum for earth model 1' [Cathles, 1975] with an adiabatic and fully nonadiabatic mantle.

can handle the different boundary conditions; thermoviscoelastic equations would be required to handle automatically the adiabatic state of the mantle, and even then the convective state of the mantle would have to be known or assumed. Cathles [1975] circumvented these problems by solving the coupled viscous and elastic responses separately using a Runge Kutta approach in which nonadiabatic density gradients for the viscous parts of the calculation can be freely inserted in the mantle or left out (adiabatic mantle). Peltier, [1976, 1982] without comment on the above complications, assumes in all his correspondence principle calculations that the elastic and viscous density profiles are identical, that is, that the mantle is fully nonadiabatic.

Adiabatic mantle conditions might result if the mantle is convecting; a fully nonadiabatic mantle would indicate that no mantle convection is taking place and that the density increase with depth is entirely due to change in mantle composition. Only a relatively small fraction of the density increase in the mantle occurs at the phase boundaries at 420 and 670 km depth. The general increase in density is due largely to self-compression. Thus much of the density increase in the mantle is adiabatic, and a fully nonadiabatic mantle (obtained by using the correspondence principle and an appropriate elastic earth model) must be considered a geologically unrealistic computational end-member.

The degree of adiabaticity of the mantle can be important in interpreting gravity anomalies in areas glacially loaded. Peltier and Wu [1982] have argued that a nonadiabatic mantle is suggested by large negative gravity anomalies in Canada and Fennoscandia. The large amount of remaining uplift suggested by these anomalies could be explained by the sluggish response of a nonadiabatic mantle to repeated, 100,000-year, glacial cycles over the last 2 m.y. Peltier and others have argued that the sluggish response of the nonadiabatic mantle can also explain recent changes in the length of day and polar wander, and perhaps help in understanding the 100,000-year glacial cycle itself (see review by Peltier [1982]).

The gravity data are, however, controversial. There is probably not a negative gravity anomaly of suitable form over Fennoscandia, and it is not certain if the gravity anomaly in central Canada is related to glacial loading (see extensive discussion by Cathles [1975, pp. 151, 265]). Recent length of day changes and polar wander could have causes other than the recent deglaciation, and the relation between isostatic response and glacial dissipation as reviewed by Peltier [1982] is admittedly speculative. Particularly in view of the importance of the question of mantle adiabaticity to broad issues such as mantle convection, as well as such issues discussed above, a test of mantle adiabaticity directly from isostatic uplift data would be useful.

In what follows, we will show through a series of comparative calculations that although the uplift responses for an adiabatic and partially nonadiabatic mantle are quite different, these differences are substantially masked by perturbations in the geoid so that the observed shoreline emergence of the two mantles is similar except near and under glaciated regions in the early stages of deglaciation. Since central areas were ice covered in the early stages of deglaciation and therefore left no emergence record, we must look near areas of major Pleistocene glaciation in the early stages of deglaciation (more than 6000 years before present) to distinguish adiabatic and nonadiabatic mantles.

Decay Spectra

The most basic way to compare the isostatic response of an adiabatic and nonadiabatic earth mantle is to compare the response as a function of time to a sudden harmonic load redistribution. The viscous response to a 1-dyn harmonic load redistribution of different order numbers for a model earth with elastic parameters described by Haddon and Bullen [1969], a 10^{22}P mantle with a 75 km thick 4 x 10^{20}P asthenosphere, and either an adiabatic or a fully nonadiabatic mantle is shown in Figure 1. The surface displacement decreases from an initial value of 1/(980 x

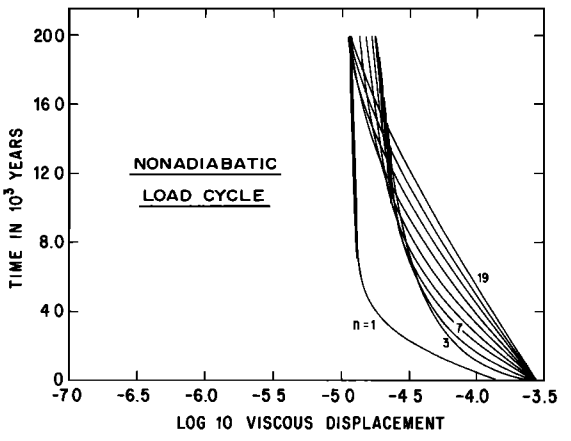

Fig. 2 Viscous decay spectrum for a fully nonadiabatic mantle as in Figure 1 but with a load cycle of 20,000 years, and every second-order number n = 1-19.

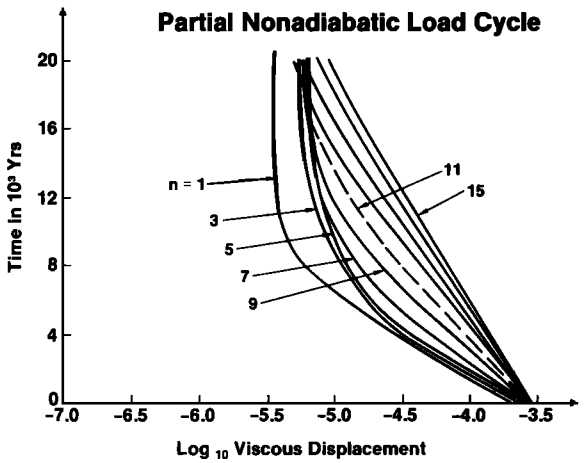

Fig. 3. Viscous decay spectrum for a partially nonadiabatic mantle with the load cycle of Figure 2.

3.315) cm, the amplitude of deformation of the upper mantle that would represent a 1 dyn load, to smaller values as time progresses. Harmonic decay for a nonadiabatic mantle is distinctly different from the adiabatic case and distinctly nonexponential. The reason for the different response in the fully nonadiabatic case is that flow in a nonadiabatic mantle deforms the density stratification which produces buoyant forces that tend to isolate flow in the upper mantle, as in a channel. The "channel" response time is much greater than the response if deep flow is allowed.

Figure 2 shows the viscous response to the removal of a 1-dyn load that has been applied for 20,000 years (about the length of major Pleistocene glaciation) and then suddenly removed, for a nonadiabatic mantle. The load cycle response of a fully nonadiabatic mantle shown in Figure 2 is quite different from the case of simple load removal shown in Figure 1, as might be expected from the slow nonadiabatic mantle adjustment indicated in Figure 1. Log decay does not start from -3.5 because the initial load has not decayed to near isostatic equilibrium in the 20,000 years the load was

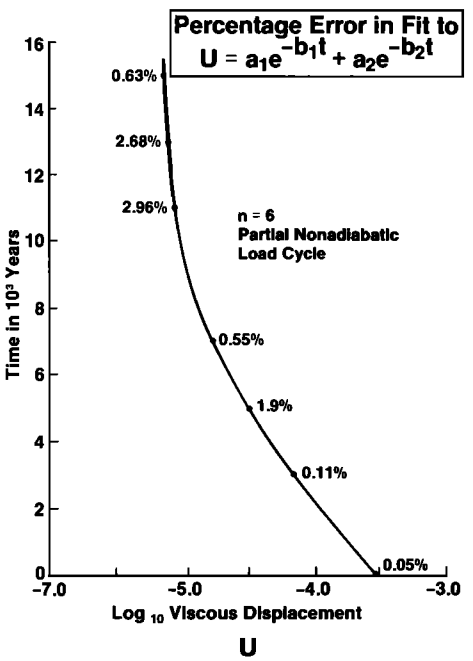

Fig. 4. Example of the fit of equation (1) to the viscous response spectra shown in Figures 1-3. Percentage error in U is shown adjacent to the fit curve (solid line) for a selected series of points.

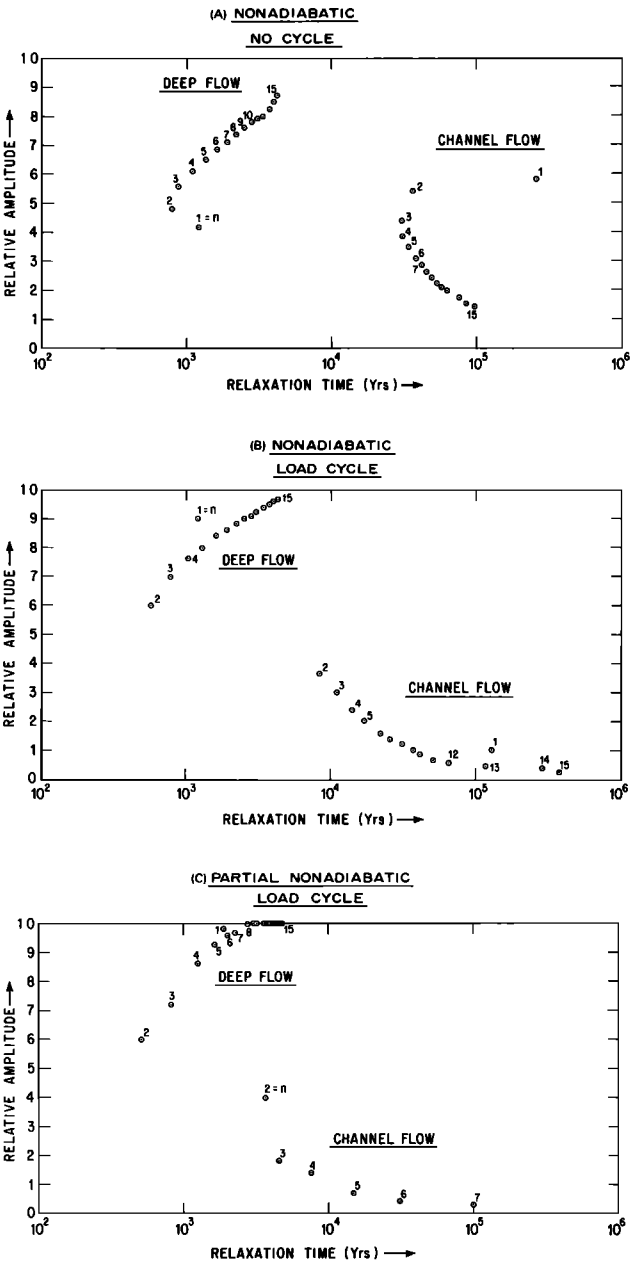

Fig.5. Relative amplitude for "deep flow" and "channel flow" viscous relaxation modes for (a) a fully nonadiabatic mantle subject to simple harmonic unloading, (b) a fully nonadiabatic mantle subject to loading for 20,000 years and then unloading (load cycle), and (c) a partially nonadiabatic mantle subject to this load cycle.

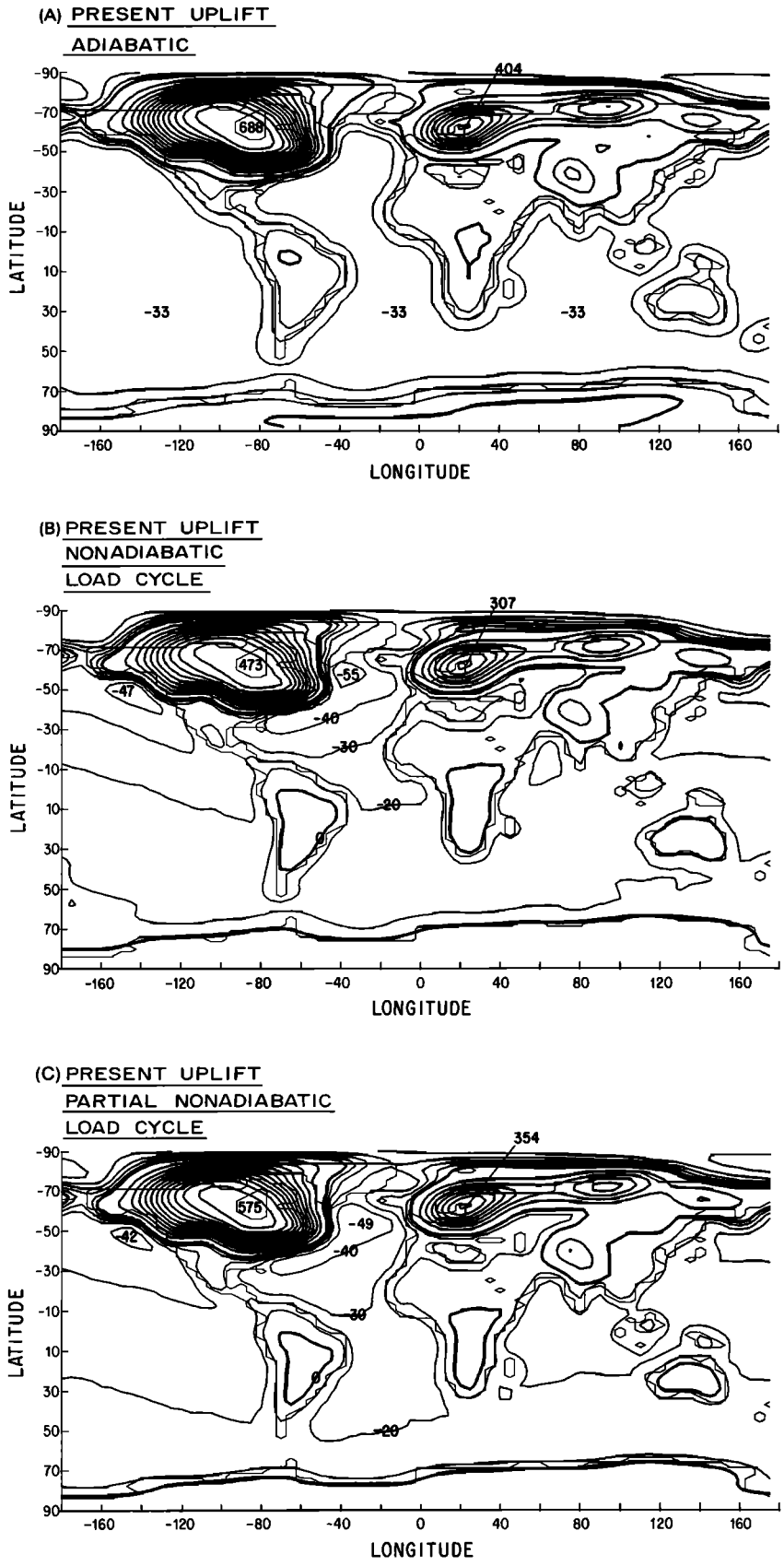

Fig. 6. Present uplift (elastic plus viscous) for (a) an adiabatic mantle, (b) a fully nonadiabatic mantle subject to a glacial load cycle, and (c) a partially nonadiabatic mantle subject to load cycle. In all cases, deglaciation was gradual and realistically mimicked the Pleistocene deglaciation [see Cathles, 1975]. The positive contour interval is 50 m, the negative 10 m.

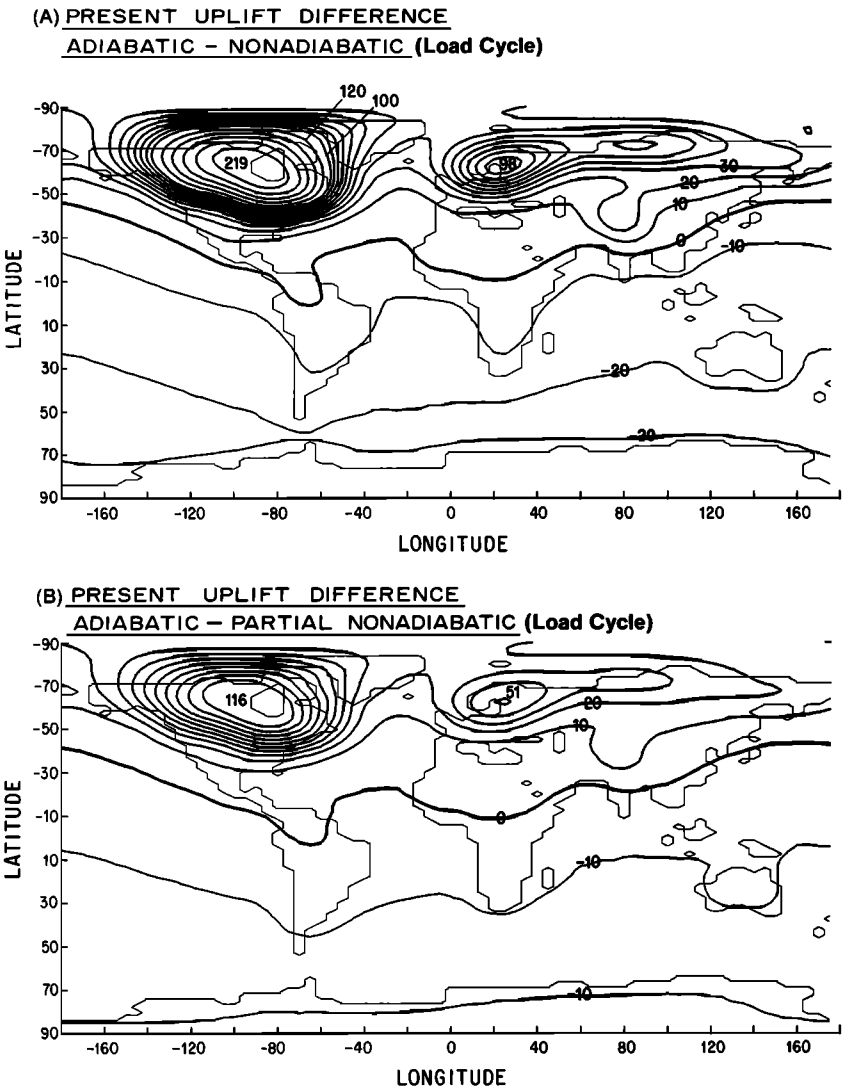

Fig. 7. The uplift difference between an adiabatic mantle (Figure 6a) and (a) a fully nonadiabatic mantle (Figure 6b) and (b) a partially nonadiabatic mantle (Figure 6c). Uplift differences in the oceans of the southern hemisphere are large enough to be easily detected in the sea level record. The contour interval is 10 m; 20 m for values greater than 100 m.

applied. The higher orders show much less curvature. The adjustment is faster because it is in part driven by energy stored in the depression of the buoyant layers that was produced during the loading part of the cycle. The response in the case of an adiabatic mantle is the same whether a load cycle is considered or not. Only the lowest order numbers show slight differences.

Figure 3 shows the response of a partially nonadiabatic mantle to the load cycle of Figure 2. The mantle in this case is nonadiabatic only between 335 and 635 km into the mantle, and the integrated nonadiabatic density jump across this zone is 0.5 g/cm^3 (see Cathles [1975, model 4, p. 110]; note that the base of the lithosphere is taken as 0 km depth). The load cycle relaxation spectrum for the partially nonadiabatic mantle (Figure 3) is still very different from that of the adiabatic mantle (Figure 1).

The most important points to be made from Figures 1-3 are that the isostatic responses of an adiabatic and either fully or partially nonadiabatic mantle are indeed quite different and that it is important in the nonadiabatic cases to take into account the fact that the Pleistocene glaciation and deglaciation was a load cycle.

For comparative purposes it is useful to fit the decay curves shown in Figures 1-3 to exponentials and plot of decay time versus order number. We fit the curves to a function

$$U = a_1 \exp(-t/c_1) + a_2 \exp(-t/c_2) \qquad (1)$$

where U is the viscous displacement. The decay of Figures 1-3 was fit to (1) using a least squares Newton-Raphson technique described by Marquardt [1963]. The quality of fit achieved with this function is shown in Figure 4.

The relative amplitudes, $a_1/(a_1+a_2)$ and $a_2/(a_1+a_2)$, are plotted versus decay time in Figure 5 for the nonadiabatic mantle models. As shown in Figure 1, harmonic deformations decay

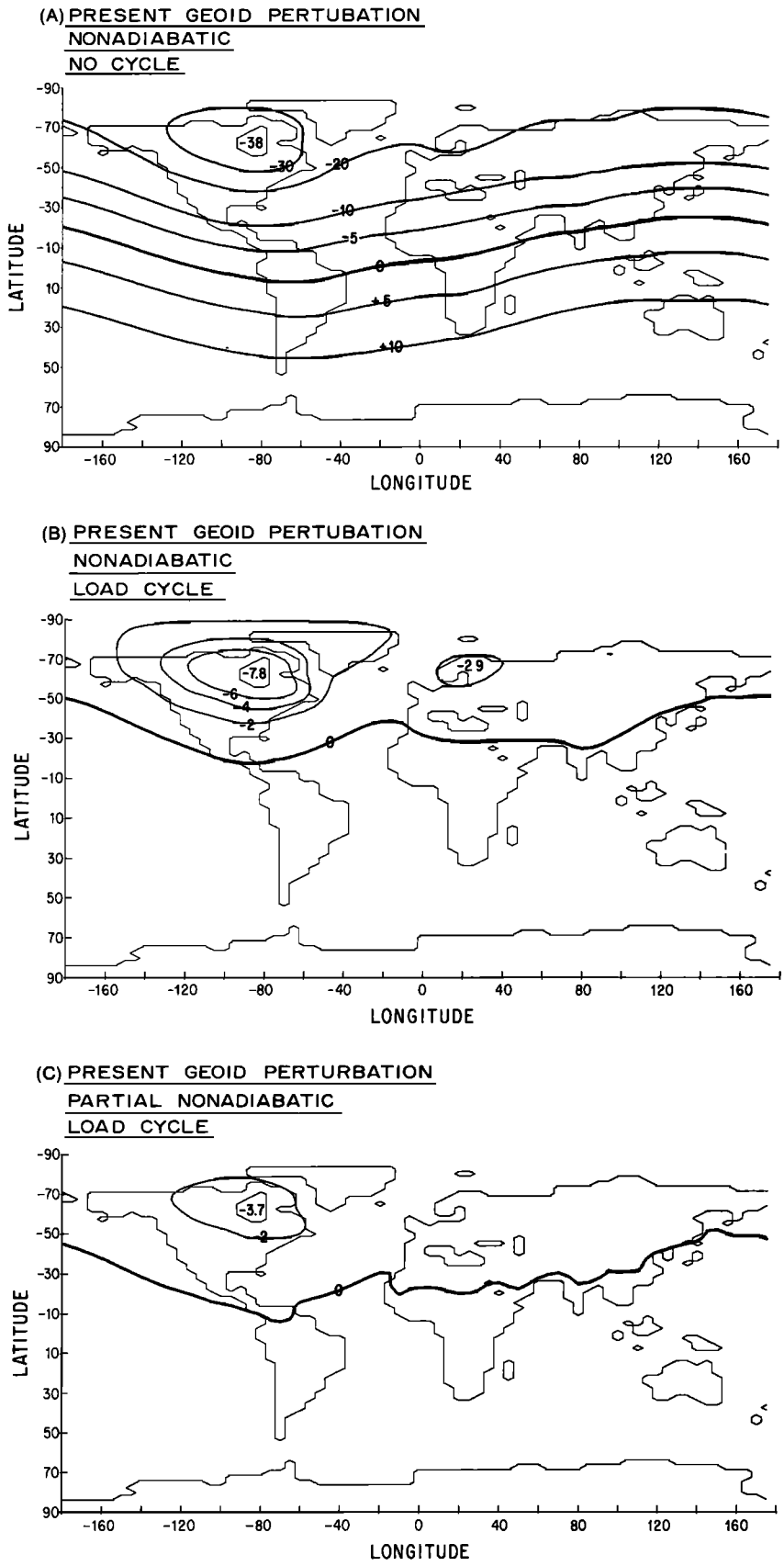

Fig. 8. The present perturbation of the geoid caused by the Pleistocene deglaciation. Figure 8b shows that the present perturbation of the geoid could be large if the mantle is fully nonadiabatic and had come to complete isostatic equilibrium under the Pleistocene load. However, Figure 8b shows that the present perturbation of even a fully nonadiabatic mantle is small if the glacial load cycle is taken into account (20,000 years loading followed by realistically gradual load removal). The present geoid perturbation is smaller still for a partially nonadiabatic mantle with load cycle (Figure 8c).

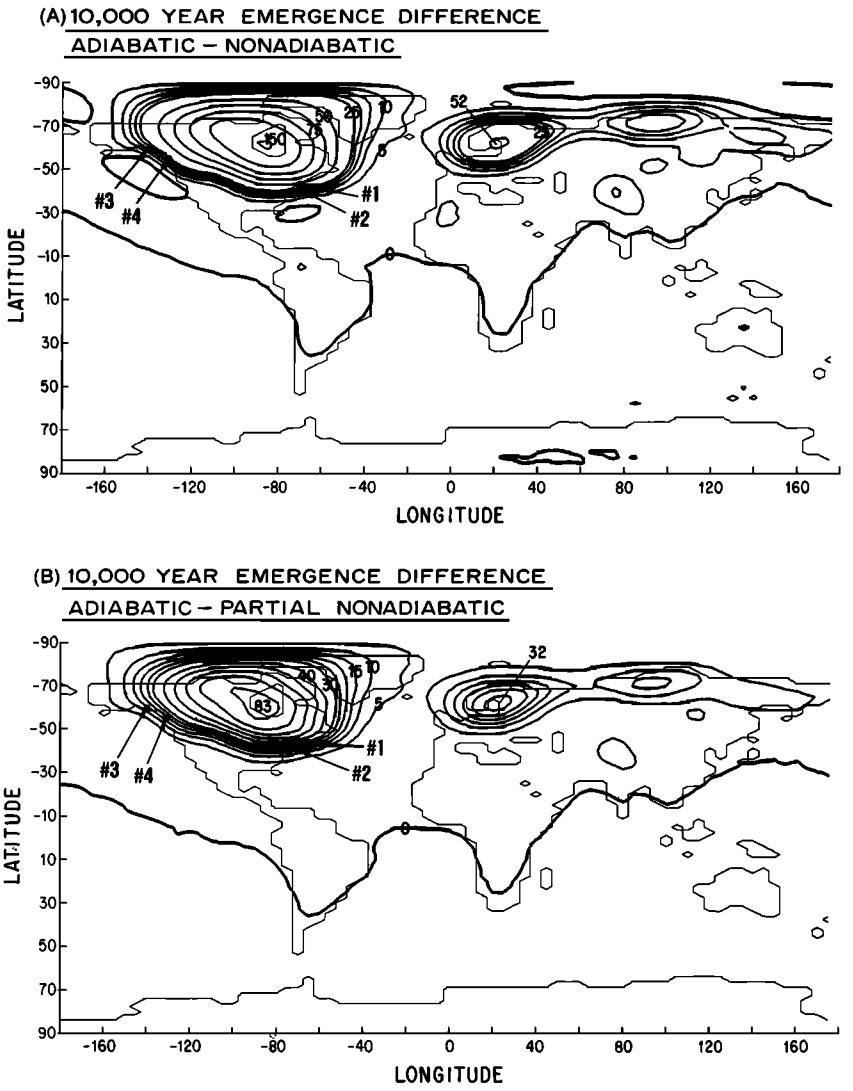

Fig. 9. Uplift curves in Figure 6 are corrected for sea level changes and geoid perturbations to give emergence curves (the calculated present elevation of past shorelines). The differences between emergence curves for an adiabatic and fully and partially nonadiabatic mantles are shown. Geoid perturbations mask differences in the oceans of the southern hemisphere (compare to Figures 7a and 7b). Adiabatic and nonadiabatic mantles are distinguished only by emergence near and under glaciated areas.

exponentially if the mantle is adiabatic; this case need not be examined by the double exponential function of (1).

As discussed earlier, the "channel flow" decay modes arise because deformation of nonadiabatic mantle layers call forth buoyant forces that tend to restrict further flow to the "channel" above these layers. The curvature in the decay spectra of Figures 1-3 (which shows up as a channel decay mode with significant amplitude in Figure 5) is the litmus of nonadiabatic mantle density gradients. Variations in viscosity with depth do not induce curvature in the decay spectra (see decay spectra of Cathles [1975, pp. 105-108]). Figure 5c shows that order numbers 2-7 are those capable of detecting nonadiabatic density gradients in a geologically reasonable, partially nonadiabatic mantle. These load harmonics are of low enough order that their relaxation behavior is not affected by any reasonable lithosphere or asthenosphere [Cathles, 1975, Figure IV-26, p. 181]. The relaxation plots of Figure 5 are similar to plots given by Peltier [1980], but we show the relative amplitudes of the modes which are critical to a determination of whether the modes are of large enough amplitude to be geologically detected. The relative proportions of the deep flow and the channel flow modes for the fully nonadiabatic mantle (Figure 5a) are in excellent agreement with Wu and Peltier [1982, Table 8, p. 465]. Our deep flow mode corresponds to Wu and Peltier's M0 mode.

Earth's Response to Pleistocene Load Redistribution

The real question, of course, is how much of a difference a nonadiabatic mantle will make in the earth's response to the redistributions of

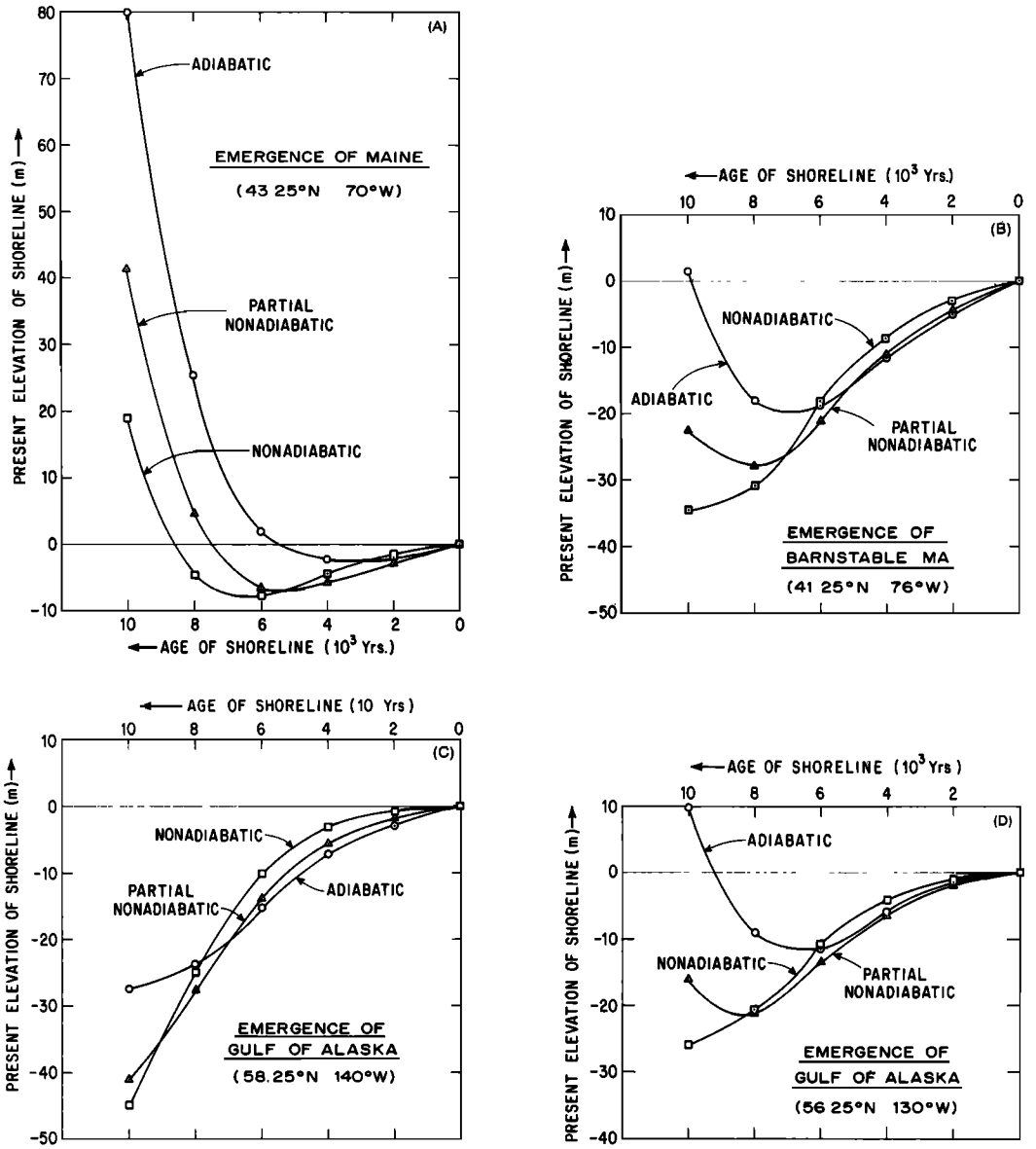

Fig. 10. Emergence curves for the four indicated locations in Figure 9. Adiabatic and nonadiabatic 10^{22}P mantles can be distinguished by emergence data near the ice edge in the early stages of deglaciation.

surface loads that occurred in the last glaciation. Figures 6-8 combine the decay spectra shown in Figures 1-3 with the elastic response and a model of the glacial history to give predicted response at the earth's surface as a function of time. Details of the method of calculation are given by Cathles [1975]. The load removal scheme of model 1 is used [Cathles, 1975, p. 110], in which T = 0 corresponds to present.

Figure 6 shows the total isostatic uplift at model time corresponding to present for an adiabatic mantle and for a fully nonadiabatic mantle and a partially nonadiabatic mantle where the load cycle is taken into consideration. There is a marked difference in the amount of uplift under the major glacier system and, more importantly, in the isostatic adjustment of the ocean basins. Notice particularly the strong troughlike depression around North America in the nonadiabatic cases.

Figure 7 shows the difference between the present uplift of an adiabatic mantle and the fully and partially nonadiabatic mantles shown in Figure 6. The differences, especially in the southern oceans, are certainly big enough to be detected.

Unfortunately, sea level curves record land emergence not actual uplift. To obtain a picture of what could be geologically measured, we must correct the uplift curves for changes in average sea level due to the meltwater influx and for changes in the geoid caused by isostatic adjustment. The present perturbation of the geoid caused by the melting of the Pleistocene glaciers is shown for three different mantle models in Figure 8. The present perturbation is large for a fully nonadiabatic mantle if the ice load cycle is not taken into account (Figure 8a) but much smaller for cases that consider load cycles.

The full history of geoid perturbation from the early stages of deglaciation through present is given for an adiabatic mantle by Cathles [1980, Figure 2]. This sequence of calculations shows that the perturbations of the geoid increase to a maximum at 8000 years before present as the glacier melted. At first, the earth was near isostatic equilibrium under the glacial load. At about 8000 years before present it was, due to the melting of the glacial ice, at its greatest isostatic disequilibrium. The pattern is similar for a 10^{22}P mantle that contains nonadiabatic density gradients, provided that the glacial load cycle is taken into account. Because the deformation of the geoid was substantial at 4000-13,000 years before present, the geoid correction to uplift data is significant despite the fact that the present perturbation of the geoid is small.

Figure 9 shows the difference between the emergence (uplift corrected for sea level changes and geoid perturbations to give the emergence of past shorelines relative to present sea level) calculated for an adiabatic and fully and partially nonadiabatic 10^{22}P mantle. Comparing Figures 9a and 9b to Figure 7a and 7b indicates that geoid corrections have eliminated differences in the oceans of the southern hemisphere nearly completely. Ocean data far removed from the ice loads cannot be used to distinguish an adiabatic from a nonadiabatic mantle. Distinguishing differences of sufficient magnitude to be discovered are to be found only near and under ice-loaded areas in the early stages of deglaciation.

This conclusion is underscored by Figure 10, which shows the emergence of four locations shown in Figure 9. Differences between emergence curves large enough to distinguish adiabatic and nonadiabatic 10^{22}P mantles are to be found near the ice edge of major glaciers in the early stages of deglaciation more than 6000-8000 years before present.

Conclusions and Discussion

The response of surface load redistribution on earth models with 10^{22}P Newtonian mantles, 75 km thick 4 x 10^{20}P Newtonian asthenospheres, and various nonadiabatic density gradients is calculated to determine whether sea level emergence since the melting of the Pleistocene ice caps can distinguish an adiabatic from a nonadiabatic or partially nonadiabatic Newtonian mantle. If the mantle is nonadiabatic, it is important to take into account the fact that Pleistocene load redistributions were load cycles. The earth did not come into isostatic equilibrium under the ice load. The earth was fully loaded by northern hemisphere glaciers for about 20,000 years, and before complete isostatic equilibrium was attained, the glacial ice melted and the perturbing load was removed. Failure to take into account the load cycle for nonadiabatic mantle models (but not adiabatic ones), as has been done in many calculations [e.g., Peltier, 1980], can lead to significantly incorrect results (Figures 1-3, 5, and 8).

As discussed by Cathles [1975, p. 85ff], nonadiabatic density gradients, either within the mantle or at the core-mantle boundary, produce distinctly curved (double or, more properly, multiple exponential) viscous displacement curves (Figures 1-3 and 5). The curvature distinguishes the nonadiabatic response from the response of an adiabatic mantle. Even with complex depth variation in mantle viscosity, viscous displacement curves in an adiabatic mantle (with no nonadiabatic discontinuity at the core mantle boundary) are single exponentials. Channel flow order numbers that can distinguish an adiabatic from a partially nonadiabatic mantle have order numbers between 2 and 7 (Figure 5c); thus broad scale uplift differences must be examined to determine the adiabaticity of the mantle.

If uplift is calculated for realistic Pleistocene glaciation and deglaciation histories, differences between adiabatic and nonadiabatic mantles in the southern hemisphere far removed from the principal ice loads appear large enough to be detected geologically (Figures 7a and 7b). However, if perturbations in the geoid are taken into account, differences in sea level emergence for adiabatic and nonadiabatic mantles are great enough for possible geological detection only near glaciated areas at times >6000 years before present (Figures 9-10). Emergence data are not recorded under areas covered by ice, so differences in these areas are not geologidally relevant. Looked at another way, information regarding the adiabaticity is in the low harmonics of the deformation spectra, but geologic information regarding the lowest harmonics is masked by gravity effects.

Confident interpretation of early emergence data from areas near the major Pleistocene glaciers will require modeling in addition to that reported here. The relaxation of high- frequency uplift components excited by local ice or water loads (which will reflect local asthenosphere and lithosphere properties) will contribute to the uplift of a particular site along with the relaxation of the low-order load harmonics that contains information regarding mantle adiabaticity. Load harmonics 2 and 7 are low enough that their decay is not affected by any reasonable lithosphere or asthenosphere, but the emergence data will reflect the decay of high- order load harmonics that are affected by local details of the load redistribution and the lithosphere and asthenosphere. Local deglaciation and earth models must therefore be constructed in order to interpret the emergence curve of a particular locality in terms of mantle adiabaticity. This requirement does not invalidate the general conclusion reached in this paper, however, that information regarding the degree of adiabaticity of the mantle resides in emergence data near glaciated areas early in the history of deglaciation. We are currently working on ways to add local details to a general earth model. Description of our approach in this regard will be the subject of a subsequent paper. Second-order contributions from redistribution of the meltwater load by geoid perturbations may also need to be accounted for, as done by Farrell and Clark [1976].

Peltier and Wu [1982] have recently emphasized the effects of many repeated glacial load cycles of 100,000-year duration on the deformational state of the earth. Figure 11 shows the effect of realistic glaciation and deglaciation cycles. In Figure 11, the 1 dyn harmonic load of order number 4 was applied gradually in a

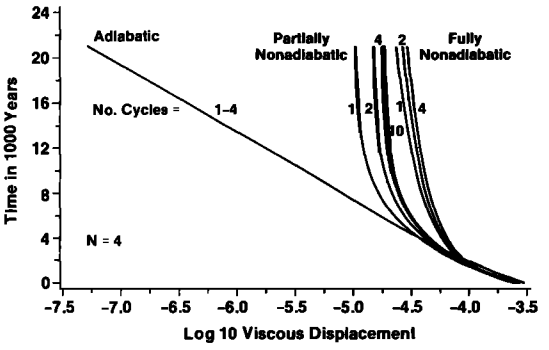

Fig. 11. Viscous response to multiple load cycles of glaciation and deglaciation. The glacial load (N =4) is applied in a linearly increasing fashion over 80,000 years and then removed. Viscous response is examined for the next 20,000 years and the load then reapplied. Multiple load cycles have no affect on the adiabatic mantle case because isostatic adjustment is nearly complete in 20,000 years. Longer- duration applied loads and multiple load cycles enhance the nonadiabatic component of the uplift response in the nonadiabatic mantle cases because, during loading, fluid adjustment in the layers above the nonadiabatic density gradients is more complete.

linearly increasing fashion for 80,000 years and then suddenly removed. Uplift over the next 20,000 years was then examined, the load applied again, 20,000 years of uplift examined, etc. Figure 11 shows the somewhat longer load application (i.e., somewhat longer than a full load for 20,000 years), and the multiple load cycles actually enhance the nonadiabatic component of the uplift response. Multiple and more realistic glaciation cycles will increase the differences shown in Figures 9-10.

A non-Newtonian mantle will have nonexponential adjustment curves similar to a Newtonian but nonadiabatic mantle [see Cathles, 1975, 1980]. The fact that apparent viscosity does not change as isostatic equilibrium is approached and the driving force reduced [Haskell, 1937] and the fact that large bulges are not produced upon glaciation and troughs upon deglaciation [Cathles, 1980] indicate that the mantle is Newtonian and that we need not be concerned about this complication.

Because the mantle appears to be Newtonian, because there are not many ways the adiabaticity of the mantle can be unambiguously probed, and because the degree of mantle adiabaticity has such fundamental implications for the styles of mantle convection that are possible, considerable theoretical and field geological efforts are justified to collect and analyze the critical early, near ice edge emergence data. We hope that calling attention to this lack and publishing maps indicating where differences between adiabatic and nonadiabatic mantles are greatest will stimulate the appropriate field studies to be carried out in parallel with the required theoretical development.

Acknowledgments. The work was carried out while both authors were at the Pennsylvania State University, and we gratefully acknowledge the support of that institution. The senior author's post doc at Penn State was financed by the Royal Council for Scientific and Industrial Research of Norway.

References

Allégre, C. J., Chemical geodynamics, Tectonophysics, 81, 109-132, 1982.

Cathles, L. M., The viscosity of the earth's mantle, Princeton University Press, Princeton, N. J., 386 pp., 1975.

Cathles, L. M., Interpretation of postglacial isostatic adjustment phenomena in terms of mantle rheology, in Earth Rheology, Isostasy and Eustasy, edited by N. A. Mörner, pp. 11-43, John Wiley, New York, 1980.

Farrell, W. E., and J. A. Clark, On postglacial sea level, Geophys. J. R. Astr. Soc., 46, 647-667, 1976.

Haddon, R. A. W., and K. E. Bullen, An earth model incorporating free earth oscillation data, Phys. Earth Planet. Inter., 2, 30-49, 1969.

Haskell, N. A., The viscosity of the asthenosphere, Am. J. Sci., 33, 22-28, 1937.

Jacobsen, S. B., and G. J. Wasserburg, The mean age of mantle and crustal reservoirs, J. Geophys. Res., 84, 7411-7427, 1979.

Love, A. E. H., Some Problems of Geodynamics, 180 pp., Cambridge University Press, New York, 1911.

Marquardt, D. W., An algorithm for least squares estimation of nonlinear parameters, J. Soc. Ind. Appl. Math., 2, 431-441, 1963.

Peltier, W. R., Glacial isostatic adjustment, II, The inverse problem, Geophys. J. R. Astron. Soc., 46, 664-706, 1976.

Peltier, W. R., Ice sheets, oceans and the earth's shape, in Earth Rheology, Isostasy and Eustasy, edited by N. A. Mörner, pp. 45-63, John Wiley, New York, 45-63, 1980.

Peltier, W. R., Dynamics of the ice age earth, Adv. Geophys., 24, 1-46, 1982.

Peltier, W. R., and J. R. Andrews, Glacial isostatic adjustment I: The forward problem, Geophys. J. R. Astron. Soc., 46, 605-646, 1976.

Peltier, W. R., and P. Wu, Mantle phase transitions and the free air gravity anomalies over Fennoscandia and Laurentia, Geophys. Res. Lett., 9, 731-734, 1982.

Wu, P., and W. R. Peltier, Viscous gravitational relaxation, Geophys. J. R. Astron. Soc., 70, 435-485, 1982.

Zindler, A., E. Jagoutz, and S. Goldstein, Nd, Sr and Pb isotopic systematics in a three-component mantle: A new perspective, Nature, 298, 519-523, 1982.

L. M. Cathles, Chevron Oil Field Research Company, P.O. Box 446, La Habra, CA 90631.

W. Fjeldskaar, SYGNA, 5850 Balestrand, Norway.

(Received May 24, 1983;
revised June 27, 1984;
accepted July 5, 1984